Proceedings of Machine Learning Research vol vvv:1–13, 2024

Dynamics Harmonic Analysis of Robotic Systems: Application in Data-Driven Koopman Modelling

Daniel Felipe Ordoñez-Apraez [1,2] DANIEL.ORDONEZ@IIT.IT
Vladimir Kostic [1] VLADIMIR.KOSTIC@IIT.IT
Giulio Turrisi [2] GIULIO.TURRISI@IIT.IT
Pietro Novelli [1] PIETRO.NOVELLI@IIT.IT
Carlos Mastalli [3] [*] C.MASTALLI@HW.AC.UK
Claudio Semini [2] CLAUDIO.SEMINI@IIT.IT
Massimiliano Pontil [1] [†] MASSIMILIANO.PONTIL@IIT.IT

[1] *Computational Statistics and Machine Learning - Istituto Italiano di Tecnologia*
[2] *Dynamic Legged Systems - Istituto Italiano di Tecnologia*
[3] *Robot Motor Intelligence – Heriot-Watt University*

Abstract

We introduce the use of harmonic analysis to decompose the state space of symmetric robotic systems into orthogonal isotypic subspaces. These are lower-dimensional spaces that capture distinct, symmetric and synergistic motions. For linear dynamics, we characterize how this decomposition leads to a subdivision of the dynamics into independent linear systems on each subspace, a property we term dynamics harmonic analysis (DHA). To exploit this property, we use Koopman operator theory to propose an equivariant deep-learning architecture that leverages the properties of DHA to learn a global linear model of system dynamics. Our architecture, validated on synthetic systems and the dynamics of locomotion of a quadrupedal robot, demonstrates enhanced generalization, sample efficiency, and interpretability, with less trainable parameters and computational costs.

Keywords: Symmetric dynamical systems, Harmonic analysis, Koopman operator, Robotics

1. Introduction

The current state-of-the-art in modeling, control, and estimation of robotic systems relies on the Lagrangian model of rigid-body dynamics, which represents the system's state as a point in the space of generalized (or minimal) coordinates. This approach has fostered the development of efficient algorithms that leverage the system's kinematic structure to enable recursive computations (Featherstone, 2007), which are ubiquitous in methods for simulation, estimation, planning, and control in robotics. However, because the model's dynamics are nonlinear, these methods need to cope with the challenges of nonlinear optimization, often through iterative local (or state-dependent) linearizations (Mayne, 1966; Li and Todorov, 2004). This can limit control policies to local minima, hinder the convergence of optimization methods, and bias the estimation of unobserved quantities.

The Koopman operator framework can potentially address these limitations by deriving globally linear models of robot dynamics, albeit in an infinite-dimensional function space (Brunton et al., 2022; Kostic et al., 2023). These models are easily leveraged by various estimation and control theory techniques (Mauroy et al., 2020), and can capture dynamic phenomena that impact system evolution but are challenging to model analytically (Asada, 2023). However, building a good data-driven model approximation in finite dimensions remains a significant machine learning challenge.

[*] Also with the Florida Institute for Human and Machine Cognition, US.
[†] Also with the Department of Computer Science, University College London, UK.

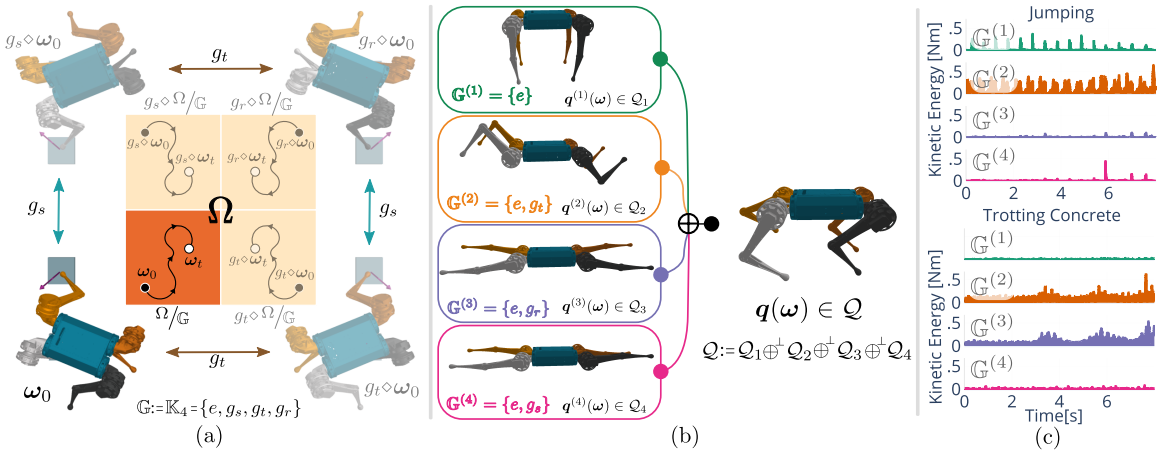

Figure 1: (a) Diagram of the discrete symmetry group $\mathbb{G} := \mathbb{K}_4$ of the mini-cheetah robot (see animation). Each symmetry $g \in \mathbb{G}$ relates states that evolve identically under physics laws, see evolution of states related by g_s. This results in the decomposition the set of states Ω into g-transformed copies of the quotient set $\Omega/\mathbb{G}$, which encompass all unique system states. (b) Isotypic decomposition of the robot's space of generalized position coordinates $\mathcal{Q}$ into isotypic subspaces: $\mathcal{Q} := \bigoplus_{i=1}^{4} \mathcal{Q}_i$. Each subspace, $\mathcal{Q}_i$ describes a space of symmetry-constrained synergistic motions. Consequently, any position configuration $\boldsymbol{q}(\boldsymbol{\omega}) \in \mathcal{Q}$, can be decomposed into projections within these subspaces: $\boldsymbol{q}(\boldsymbol{\omega}) := \bigoplus_{i=1}^{4} \boldsymbol{q}^{(i)}(\boldsymbol{\omega})$ (see animation). (c) Kinetic energy distribution across isotypic subspaces for two gait/motion trajectories in the real-world: jumping and trotting (see animation). Both gaits primarily evolve within one or two lower-dimensional isotypic subspaces, with less significant subspaces engaged temporarily during disturbances.

In this work, we show that, by exploiting the system's symmetries, our approach improves the model' interpretability, sample efficiency, and quality, whilst reducing trainable parameters and computational cost. Although we focus on robotics, our proposed modeling framework applies to any dynamical systems with discrete symmetry groups.

In robotics, the symmetries we aim to exploit are known as morphological symmetries (Ordonez-Apraez et al., 2023). These are discrete symmetry groups that capture the equivariance of the robot's dynamics, arising from the duplication of rigid bodies and kinematic chains (see Fig. 1-a). Inspired by the use of harmonic analysis of discrete symmetry groups in physics (Dresselhaus et al., 2007), we present the first application of these principles in robotics. Specifically, we employ the isotypic decomposition (Thm. 1) to partition the state space of symmetric robotic systems into isotypic subspaces (see Fig. 1-b). This allows us to represent any system motion (e.g., different locomotion gaits, or manipulation movements) as a superposition of simpler, symmetric, synergistic motions[1]; each evolving in a distinct isotypic subspace (see Fig. 1-c). Moreover, we demonstrate that the isotypic decomposition leads to the partitioning of any (local or global) linear model of the system's dynamics into independent linear subsystems, each characterizing the dynamics of an isotypic subspace. An advantage of this is that the Koopman model can be decomposed into independent Koopman submodels, each capturing the dynamics of a specific type of synergistic motion on an isotypic subspace. This represents a significant improvement in interpretability.

Contributions In summary, we make the following contributions: **1)** We introduce the use of harmonic analysis of discrete symmetry groups to robotics. **2)** We propose the concept of dynamics harmonic analysis (DHA), illustrating how local/global linear dynamics models decompose into linear subsystems within isotypic subspaces (Sec. 3). **3)** Leveraging on DHA, we propose the equiv-

1. These are the robotics analog of normal vibrational modes in molecular dynamics, see (Dresselhaus et al., 2007, 8.3)

ariant Dynamics Autoencoder (eDAE), a deep-learning architecture to approximate the Koopman operator (Sec. 4), and report its strong performance on synthetic and robotics systems (Sec. 5). **4)** We provide an open-access repository enabling the application of harmonic analysis to a library of symmetric robots and the use of the eDAE architecture.

Related work For data-driven approximation of Koopman operators Noé and Nuske (2013), Lusch et al. (2018), and Kostic et al. (2023) introduce symmetry-agnostic deep learning algorithms, which can be adapted to exploit DHA, as proposed in Sec. 4. In the spirit of our work, Steyert (2022) studies the operator's structure for systems evolving on manifolds, i.e. featuring continuous symmetry groups. For discrete symmetry groups, Salova et al. (2019) leverage the operator's block-diagonal structure after using harmonic analysis on a non-learnable dictionary of observable functions, to model duffing oscillators. Lastly, Mesbahi et al. (2019); Sinha et al. (2020) provide theoretical analysis on the structure of the operator for modeling symmetric dynamical systems.

In Robotics, the use of Koopman operator theory for modeling, estimation, and control is gaining traction. This interest stems from the versatility of the resulting models, which are compatible with a wide array of control theory and state estimation techniques, including optimal and robust control (Korda and Mezić, 2018; Folkestad and Burdick, 2021; Zhang et al., 2022), active learning (Abraham and Murphey, 2019), system identification and observer synthesis (Bruder et al., 2020; Surana, 2020). However, symmetries have not been exploited in any of these Koopman-based modeling, estimation, and control approaches.

2. Preliminaries

Here we overview background material on dynamical systems modeling, Koopman models, and harmonic analysis, needed to address the modeling of symmetric dynamical systems in Sec. 3.

Modeling of dynamical systems Differentiating between a dynamical system and its numerical model is essential in our analysis. A dynamical system abstracts real-world evolving phenomena, like a robot's movement in an environment. In contrast, numerical models *approximate* the system's dynamics as the time evolution of points (representing the system's state) in a vector space. A dynamical system is typically defined by a tuple $(\Omega, \mathbb{T}, \Phi_\Omega)$, where Ω is the abstract set of system states $\boldsymbol{\omega} \in \Omega$, the set $\mathbb{T}$ represents time (usually $\mathbb{T} = \mathbb{N}_0$ for discrete, or $\mathbb{T} = \mathbb{R}_+$ for continuous systems), and $\Phi_\Omega \colon \Omega \times \mathbb{T} \to \Omega$ is the evolution map. It determines the system state $\boldsymbol{\omega}_t$ at any given time t as a function of the current state and time, namely, $\boldsymbol{\omega}_t := \Phi_\Omega(\boldsymbol{\omega}_0, t),\ t \in \mathbb{T}, \boldsymbol{\omega}_0 \in \Omega$.

Defining a numerical model of a dynamical system involves identifying a state representation vector valued function $\boldsymbol{x} = [x_1, \dots, x_\ell]$, where the components, $x_j : \Omega \to \mathbb{C},\ j = 1, \dots, \ell$, are observable functions that measure a relevant scalar quantity from the state (e.g., kinetic energy, joint position/velocity). This allows to represent the system state as a point in the model's vector space $\boldsymbol{x}(\boldsymbol{\omega}) \in \mathcal{X}$. Then, the system's evolution, represented as a trajectory $(\boldsymbol{x}(\boldsymbol{\omega}_t))_{t\in\mathbb{T}}$, can be approximately modeled by a learned/optimized evolution map $\Phi_\mathcal{X}(\boldsymbol{x}(\boldsymbol{\omega}_0), t) \approx \boldsymbol{x}(\boldsymbol{\omega}_t)$. If the state representation $\boldsymbol{x} : \Omega \to \mathcal{X}$ is injective, the quality (or optimality) of the model $(\mathcal{X}, \mathbb{T}, \Phi_\mathcal{X})$ is quantified by the state prediction error over a prediction horizon $H \in \mathbb{T}$ (Mezić, 2021), i.e.,

$$\text{err}_{\boldsymbol{\omega}_0, H}(\boldsymbol{x}, \Phi_\mathcal{X}) := \int_0^H d(\Phi_\mathcal{X}(\boldsymbol{x}(\boldsymbol{\omega}_0), t),\ \boldsymbol{x}(\boldsymbol{\omega}_t))^2 dt. \tag{1}$$

where $d(\cdot, \cdot)$ measures distance between points in $\mathcal{X}$, considering geodesic distances if $\mathcal{X}$ has a manifold structure. Note that while modeling error can be locally minimal for specific $\boldsymbol{\omega}_0$ and $H \in \mathbb{T}$, optimal models exhibit uniformly small errors across all states and horizons.

Linear models and the Koopman operator Linear models offer numerous numerical and theoretical advantages, making them fundamental to dynamical systems and control theory. They have an evolution map characterized by the dynamics of an autonomous linear system, $\Phi_{\mathcal{X}}(\boldsymbol{x}(\boldsymbol{\omega}), {}_{\Delta}t) := \mathsf{X}_{{}_{\Delta}t}\boldsymbol{x}(\boldsymbol{\omega}),\ \boldsymbol{\omega} \in \Omega, {}_{\Delta}t \in \mathbb{T}$, where $\mathsf{X}_{{}_{\Delta}t} \colon \mathcal{X} \to \mathcal{X}$ is a linear operator/matrix that depends on ${}_{\Delta}t$. Since $(\mathsf{X}_{{}_{\Delta}t})_{{}_{\Delta}t \in \mathbb{T}}$ forms a semigroup, we usually identify the flow $\Phi_{\mathcal{X}}$ with the generator of the semigroup X defined as $\mathsf{X} := \mathsf{X}_1$ when $\mathbb{T} = \mathbb{N}_0$, or as $\mathsf{X} := \lim_{{}_{\Delta}t \to 0^+}(I - \mathsf{X}_{{}_{\Delta}t})/{}_{\Delta}t$ when $\mathbb{T} = \mathbb{R}_+$. Moreover, via the spectral decomposition of X, the flow can be decomposed into eigenvectors with dynamics determined by a scalar eigenvalue, allowing the interpretation of dynamics.

Although most dynamical systems of interest in robotics have been historically modeled with nonlinear analytic dynamics, one can also devise an optimal linear model in an infinite-dimensional space. This idea, originating from the seminal work of Koopman and Markov (Lasota and Mackey, 1994), proposes to represent the state as a function in a *space of functions* $\mathcal{X}$, and model the dynamics with a map, defined by the flow Φ_Ω and a time step $\Delta t \in \mathbb{T}$, which takes any function $x \in \mathcal{X}$ to $x(\Phi_\Omega(\cdot, \Delta t))$. Whenever the map's image is in the same space, we have a well-defined linear operator $\mathsf{X}_{{}_{\Delta}t} \colon \mathcal{X} \to \mathcal{X}$, known as the *Koopman operator*, given by

$$[\mathsf{X}_{{}_{\Delta}t}\, x](\boldsymbol{\omega}) := x(\Phi_\Omega(\boldsymbol{\omega}, {}_{\Delta}t)),\ x \in \mathcal{X},\ \boldsymbol{\omega} \in \Omega. \tag{2}$$

When the dynamic is stochastic (i.e., $\boldsymbol{\omega}_t$ are random variables), one should take the conditional expectation w.r.t. $\boldsymbol{\omega}$ of the r.h.s. of eq. (2) to properly define $\mathsf{X}_{{}_{\Delta}t}$. In this case, the operator is denoted as *forward transfer operator* (Meyn and Tweedie, 1993). A key motivation for the use of these operators is the interpretability of the dynamics arising from its spectral decomposition. Namely, if $\mathsf{X}_{{}_{\Delta}t}\psi = \lambda\psi$, that is $\psi \in \mathcal{X}$ is a Koopman eigenfunction corresponding to eigenvalue $\lambda \in \mathbb{C}$, then eq. (2) implies $\psi(\boldsymbol{\omega}_{k\Delta t}) = \lambda^k \psi(\boldsymbol{\omega}_0)$. Thus, the representation $\psi \colon \Omega \to \mathbb{C}$ is invariant under the flow, which becomes a scalar wave with amplitude $|\lambda|^{1/{}_{\Delta}t}$ and frequency $\mathrm{Arg}(\lambda)/(2\pi{}_{\Delta}t)$.

The requirement for space $\mathcal{X}$ to be invariant under the flow Φ_Ω is the characteristic that often renders it infinite-dimensional. To approximate this optimal linear model in finite dimensions requires identifying a suitable state representation $\boldsymbol{x} : \Omega \to \mathcal{X}$, characterizing a finite-dimensional subspace (spanned by a subset of observable functions), and empirically approximating the transfer/Koopman operator in this space. As we will discuss in Sec. 4, machine learning, particularly deep learning, can aid in finding suitable state representations (Lusch et al., 2018; Kostic et al., 2023).

For simplicity, in the following, we specify $\mathbb{T}$ and $\mathcal{X}$ only when necessary. Hence, a dynamical system will be denoted by Φ_Ω, its numerical model as $\Phi_{\mathcal{X}}$, or as X if it is a linear model.

Symmetry groups and their representations We next introduce the notion of symmetries that are used in Sec. 3 in the context of a dynamical systems. Symmetries are defined as bijections on the state set Ω. The action of a symmetry transformation g on any state $\boldsymbol{\omega} \in \Omega$ is a map $\diamond : \mathbb{G} \times \Omega \to \Omega$ to a symmetric state $g \diamond \boldsymbol{\omega} \in \Omega$ (see Fig. 1-a). A set of symmetry transformations forms a group $\mathbb{G} = \{e, g_1, g_2, \dots\}$, that is closed under *composition:* $g_1 \circ g_2 \in \mathbb{G}$ for all $g_1, g_2 \in \mathbb{G}$, and *inversion:* $g^{-1} \in \mathbb{G} \mid g \in \mathbb{G}$ such that $g^{-1} \circ g = e$, where e denotes the identity transformation and $(\circ)$ is the binary composition operation on $\mathbb{G}$.

Given that we study numerical models in both finite-dimensional (Euclidean) spaces and infinite-dimensional function spaces, we assume $\mathcal{X}$ to be a separable Hilbert space to accommodate both scenarios. Thus, we rely on the conventional concepts of inner product, orthogonality, and countably many basis elements. Consequently, symmetry transformations on $\mathcal{X}$ are defined via a unitary group representation $\rho_{\mathcal{X}} : \mathbb{G} \to \mathbb{U}(\mathcal{X})$, mapping each $g \in \mathbb{G}$ to its representation as a unitary ma-

trix/operator transformation $\rho_{\mathcal{X}}(g) \in \mathbb{U}(\mathcal{X}) : \mathcal{X} \to \mathcal{X}$. Thus, for any point $\boldsymbol{x} \in \mathcal{X}$, the action of any $g \in \mathbb{G}$ is expressed as $g \diamond \boldsymbol{x} := \rho_{\mathcal{X}}(g)\boldsymbol{x} \in \mathcal{X}$. If $\rho_{\mathcal{X}}(g)$ exists, we say that $\mathcal{X}$ is a symmetric space.

A map $f : \mathcal{X} \to \mathcal{X}'$ between two symmetric spaces is said to be $\mathbb{G}$-equivariant if $f(\rho_{\mathcal{X}}(g)\boldsymbol{h}) = \rho_{\mathcal{X}'}(g)f(\boldsymbol{h})$, and $\mathbb{G}$-invariant if $f(\boldsymbol{h}) = f(\rho_{\mathcal{X}}(g)\boldsymbol{h})$, for all $g \in \mathbb{G}$. These transformations are dependent on the chosen basis of $\mathcal{X}$. Applying a change of basis $\mathsf{Q} \in \mathbb{U}(\mathcal{X})$ implies a different representation of a point $\boldsymbol{x}$ in the new basis $\boldsymbol{x}' = \mathsf{Q}\boldsymbol{x}$, and a new group representation $\rho'_{\mathcal{X}}(\cdot) = \mathsf{Q}\rho_{\mathcal{X}}(\cdot)\mathsf{Q}^*$. Group representations related by a change of basis are equivalent, denoted as $\rho_{\mathcal{X}} \sim \rho'_{\mathcal{X}}$.

Isotypic decomposition and its basis Our use of harmonic analysis is linked with the decision to work in a specific basis for the modeling space $\mathcal{X}$, the *isotypic basis*. In this basis, the unitary group representations $\rho_{\mathcal{X}}$ decomposes into a block-diagonal sum of multiple copies (*multiplicities*) of the group's k unique irreducible representations (*irrep*) $\{\bar{\rho}_i\}_{i=1}^{k}$. These are the indivisible building blocks of any group representation of $\mathbb{G}$. Each $\bar{\rho}_i : \mathbb{G} \to \mathbb{U}(\mathcal{H}_i)$, describes a unique symmetry pattern, characterized by a subset of symmetry transformations within the broader group structure. The space $\mathcal{H}_i$ associated to each *irrep* is the smallest finite-dimensional space capable of expressing the *irrep* symmetry pattern (e.g., a 1-dimensional space for a reflection symmetry, or a 2-dimensional space for 2-dimensional rotational symmetry). These representations are called irreducible because the spaces $\mathcal{H}_i$ have no non-trivial invariant subspace to the actions of $\mathbb{G}$. That is, if $\mathcal{V}$ is a subspace of $\mathcal{H}_i$ and $\bar{\rho}_i(g)\mathcal{V} \subset \mathcal{V}$ for every $g \in \mathbb{G}$, then either $\mathcal{V} = \{0\}$ or $\mathcal{V} = \mathcal{H}_i$.

The value of the isotypic basis lies in the fact that it allows decomposing the modeling space $\mathcal{X}$ into an orthogonal sum of isotypic subspaces. Each subspace reflects a unique symmetry pattern of one of the group's *irreps*, hence the term *iso-typic* or *same-type*. This is a pivotal result in abstract harmonic analysis, succinctly captured by the Peter-Weyl Theorem, see (Knapp, 1986, Thm 1.12) and (Golubitsky et al., 2012, Thm-2.5).

Theorem 1 (Isotypic decomposition) *Let $\mathbb{G}$ be a compact symmetry group and $\mathcal{X}$ be a symmetric separable Hilbert space with an associated unitary group representation $\rho_{\mathcal{X}} : \mathbb{G} \to \mathbb{U}(\mathcal{X})$. Then, there exists a finite number of unique finite-dimensional subspaces $\mathcal{H}_i \subset \mathcal{X}$ and irreducible representations $\bar{\rho}_i : \mathbb{G} \to \mathbb{U}(\mathcal{H}_i)$, $i \in [1, k]$ and at most countably many subspaces $\mathcal{X}_{i,j}$, $j \in [1, m_i]$ each isometrically isomorphic to $\mathcal{H}_i$, such that $\rho_{\mathcal{X}} \sim \rho_{\mathcal{X}_1} \oplus \rho_{\mathcal{X}_2} \oplus \cdots \oplus \rho_{\mathcal{X}_k}$, where $\rho_{\mathcal{X}_i} \sim \bigoplus_{j=1}^{m_i} \bar{\rho}_i$ is a unitary group representation acting on an isotypic subspace $\mathcal{X}_i = \mathcal{X}_{i,1} \oplus^{\perp} \cdots \oplus^{\perp} \mathcal{X}_{i,m_i}$, $i = [1, k]$, implying isotypic decomposition $\mathcal{X} = \mathcal{X}_1 \oplus^{\perp} \mathcal{X}_2 \oplus^{\perp} \cdots \oplus^{\perp} \mathcal{X}_k$.*

3. Symmetries of dynamical systems

In the context of dynamical systems, a symmetry is a state transformation that results in another functionally equivalent state under the governing dynamics. In other words, states related by a symmetry transformation will exhibit similar evolution when subjected to identical forces. From a modeling perspective, symmetries provide a valuable geometric bias, as identifying the dynamics of a single state suffices to capture the dynamics of all of its symmetric states.

Definition 1 (Symmetric dynamical systems) *A dynamical system $(\Omega, \mathbb{T}, \Phi_\Omega)$ is $\mathbb{G}$-symmetric, if $\mathbb{G}$ is a symmetry group of the set of states Ω, and the system's evolution map is $\mathbb{G}$-equivariant, i.e.,*

$$\Phi_\Omega(g \diamond \boldsymbol{\omega}, t) = g \diamond \Phi_\Omega(\boldsymbol{\omega}, t), \quad g \in \mathbb{G}, t \in \mathbb{T}. \tag{3}$$

The symmetry group of Ω defines an equivalence relationship between any state $\boldsymbol{\omega} \in \Omega$ and its set of symmetric states, denoted $\mathbb{G}\boldsymbol{\omega} = \{g \diamond \boldsymbol{\omega} | g \in \mathbb{G}\}$. Given the $\mathbb{G}$-equivariance of the dynamics

Φ_Ω, this equivalence implies that a set of symmetric states $\mathbb{G}\boldsymbol{\omega}$ will evolve along a unique trajectory of motion, up to a symmetry transformation $g \in \mathbb{G}$ (see Fig. 1-a). When the symmetry group is discrete (or finite), the state set Ω decomposes into a union of symmetry-transformed copies of the quotient set $\Omega/\mathbb{G}$, which contains the system's unique states, that is $\Omega = \cup_{g\in\mathbb{G}}\{g \diamond \Omega/\mathbb{G}\}$ (see Fig. 1-a). From a modeling perspective, it suffices to model the dynamics within the quotient set to generalize to the entire state set Ω.

Modeling symmetric dynamical systems When designing a numerical model $\Phi_\mathcal{X}$ for a symmetric dynamical system, it is crucial to ensure that the modeling space $\mathcal{X}$ inherits the group structure of Ω. This can be achieved by making the space invariant under the action of the group elements, i.e., $\boldsymbol{x}(g\diamond(\cdot)) \in \mathcal{X}$ for all $g \in \mathbb{G}$, enabling the existence of a group representation $\rho_\mathcal{X} : \mathbb{G} \to \mathbb{U}(\mathcal{X})$. The significance of this design choice lies in the fact that the equivalence between symmetric states is translated into the corresponding equivalence of their representations in the modeling space:

$$\mathbb{G}\boldsymbol{\omega} := \{g\diamond\boldsymbol{\omega} \mid \forall\, g \in \mathbb{G}\} \iff \mathbb{G}\boldsymbol{x}(\boldsymbol{\omega}) := \{g\diamond\boldsymbol{x}(\boldsymbol{\omega}) = \rho_\mathcal{X}(g)\boldsymbol{x}(\boldsymbol{\omega}) = \boldsymbol{x}(g\diamond\boldsymbol{\omega}) \mid \forall\, g \in \mathbb{G}\} \quad (4)$$

The symmetric structure of $\mathcal{X}$ allows its decomposition into g-transformed copies of a quotient space $\mathcal{X}/\mathbb{G}$. This is a practical tool in data-driven applications, mitigating the effects of the curse of dimensionality (Higgins et al., 2022). As the following result shows, it also narrows the search space for the evolution map $\Phi_\mathcal{X}$ to the space of $\mathbb{G}$-equivariant ones.

Proposition 2 (Optimal models of $\mathbb{G}$-symmetric systems) *Let Φ_Ω be a $\mathbb{G}$-symmetric dynamical system and $\Phi_\mathcal{X}$ its optimal model. If $\mathcal{X}$ is a $\mathbb{G}$-symmetric space, $\Phi_\mathcal{X}$ is $\mathbb{G}$-equivariant.*

Proof Let $\mathbb{G}\boldsymbol{\omega}$ be any set of symmetric states and $\mathbb{G}\boldsymbol{x}(\boldsymbol{\omega})$ their symmetric representations on $\mathcal{X}$. Then, any non $\mathbb{G}$-equivariant evolution map $\bar{\Phi}_\mathcal{X}$ will result in different prediction errors for the states $\mathbb{G}\boldsymbol{\omega}$. Therefore, we can identify the state with the minimum prediction error $\hat{g}\diamond\boldsymbol{\omega} \in \mathbb{G}\boldsymbol{\omega}$, given $\hat{g} = \arg\min_{g\in\mathbb{G}} \text{err}_{g\diamond\boldsymbol{\omega}}(\boldsymbol{x}, \bar{\Phi}_\mathcal{X})$ (eq. (1)). Then, we can define the new map $\Phi_\mathcal{X}(\boldsymbol{x}(g\diamond\boldsymbol{\omega}), t) := (g\circ\hat{g}^{-1})\diamond\bar{\Phi}_\mathcal{X}(\boldsymbol{x}(\hat{g}\diamond\boldsymbol{\omega}), t)) \mid \forall\, g \in \mathbb{G}, t \in \mathbb{T}$ which appropriately reproduces the predicted evolution of $\hat{g}\diamond\boldsymbol{\omega}$ for all symmetric states. Note that, $\text{err}_{g\diamond\boldsymbol{\omega}}(\boldsymbol{x}, \Phi_\mathcal{X}) \leq \text{err}_{g\diamond\boldsymbol{\omega}}(\boldsymbol{x}, \bar{\Phi}_\mathcal{X})$ for all $g \in \mathbb{G}$. By iteratively repeating this process for all $\boldsymbol{\omega} \in \Omega/\mathbb{G}$ the resultant map will be $\mathbb{G}$-equivariant. ■

Consistent with Def. 1, we denote models $(\mathcal{X}, \Phi_\mathcal{X})$ that possess a $\mathbb{G}$-symmetric modeling state space $\mathcal{X}$ and a $\mathbb{G}$-equivariant evolution map as $\mathbb{G}$-symmetric models. A familiar example is the Lagrangian model of rigid-body dynamics. Since, for $\mathbb{G}$-symmetric robotic systems (e.g., the mini-cheetah in Fig. 1), the modeling space $\mathcal{X} = \mathcal{Q} \times \mathcal{T}_\boldsymbol{q}\mathcal{Q}$, defined by the space of generalized position $\mathcal{Q}$ and velocity $\mathcal{T}_\boldsymbol{q}\mathcal{Q}$ coordinates, is a symmetric vector space (Ordonez-Apraez et al., 2023, III). It has a group representation $\rho_\mathcal{X} := \rho_\mathcal{Q} \oplus \rho_{\mathcal{T}_\boldsymbol{q}\mathcal{Q}}$, which describes the transformations shown in Fig. 1-a. Furthermore, the evolution map $\Phi_\mathcal{X}$, defined by the standard Euler-Lagrangian equations of motion, exhibits $\mathbb{G}$-equivariance (Lanczos, 2012, VII.2).

Another advantage of non-linear or linear $\mathbb{G}$-symmetric models is the decomposition of the modeling state space into k isotypic subspaces $\mathcal{X} = \bigoplus_{i=1}^{k}\mathcal{X}_i$ (refer to Thm. 1). This enables the projection of entire motion trajectories $(\boldsymbol{x}(\boldsymbol{\omega}_t))_{t\in\mathbb{T}}$ onto each isotypic subspace $\boldsymbol{x}(\boldsymbol{\omega}_t) := \boldsymbol{x}^{(1)}(\boldsymbol{\omega}_t) \oplus^\perp \cdots \oplus^\perp \boldsymbol{x}^{(k)}(\boldsymbol{\omega}_t)$. Since each $\mathcal{X}_i$ is a lower-dimensional space with a reduced number of symmetries, the trajectory's decomposition entails its characterization as a superposition of distinct lower-dimensional synergistic motion trajectories $(\boldsymbol{x}^{(i)}(\boldsymbol{\omega}_t))_{t\in\mathbb{T}} \mid \boldsymbol{x}^{(i)}(\boldsymbol{\omega}_t) \in \mathcal{X}_i$, each constrained to feature the subset of symmetries of $\mathcal{X}_i$ (see Fig. 1-b). This understanding is instrumental in characterizing different system behaviors, such as different locomotion gaits or manipulation tasks, through their lower-dimensional projections onto each isotypic subspace, as detailed in Fig. 1-c.

The utility of the isotypic decomposition is amplified for $\mathbb{G}$-symmetric *linear* models, X. For these models, the decomposition of the modeling state space $\mathcal{X} = \bigoplus_{i=1}^{k} \mathcal{X}_i$ additionally implies the decomposition of the dynamics into k independent linear subsystems $\mathsf{X} = \bigoplus_{i=1}^{k} \mathsf{X}_i$, each evolving the state projections into isotypic subspaces independently. This property stems from Schur's Lemma, a standard result in harmonic analysis (Knapp, 1986, Prop 1.5), which essentially states that nontrivial $\mathbb{G}$-equivariant linear maps between vector spaces associated with *irreps* of different types do not exist, i.e., $\mathsf{X}_{i\to j} = \mathbf{0} \mid \mathsf{X}_{i\to j} : \mathcal{X}_i \to \mathcal{X}_j, \forall\, i \neq j$. Thus, for $\mathbb{G}$-symmetric linear models, projecting the flow onto the isotypic subspaces yields the following result, essentially stated in (Golubitsky et al., 2012, Thm 3.5) for finite-dimensional spaces:

Theorem 3 (Isotypic decomposition of symmetric linear models) *Let $\mathbb{G}$ be a finite group, X a $\mathbb{G}$-symmetric linear model on $\mathcal{X}$, and $\mathcal{X} = \bigoplus_{i=1}^{k} \mathcal{X}_i$ be the state space isotypic decomposition. Then X is block-diagonal $\mathsf{X} = \bigoplus_{i=1}^{k} \mathsf{X}_i$, where each block $\mathsf{X}_i : \mathcal{X}_i \to \mathcal{X}_i$ is a $\mathbb{G}$-equivariant linear map characterizing the dynamics of each isotypic subspace. Consequently, model X decomposes into sub-models X_i, $i \in [1, k]$ where the modeling error satisfies $\operatorname{err}_{\boldsymbol{\omega}_0,t}(\boldsymbol{x}, \mathsf{X}) = \sum_{i=1}^{k} \operatorname{err}_{\boldsymbol{\omega}_0,t}(\boldsymbol{x}^{(i)}, \mathsf{X}_i)$.*

This result has two primary applications in robot dynamics modeling. The first involves decomposing local linear models resulting from local (or state-dependent) linearizations of nonlinear dynamical models. These are widely used in the iLQR (Li and Todorov, 2004) and DDP (Mayne, 1966) algorithms, which are instrumental for trajectory optimization (Tassa et al., 2014; Mastalli et al., 2020), and state estimation (Alessandri et al., 2003; Kobilarov et al., 2015). For these methods, the decomposition of the local linear dynamics facilitates the parallel optimization of the k local linear sub-models, presenting a promising direction for future research. The second application pertains to the decomposition for $\mathbb{G}$-symmetric Koopman models, which we discuss next.

Dynamic harmonic analysis For a $\mathbb{G}$-symmetric dynamical system Φ_Ω, an injective state representation $\boldsymbol{x} : \Omega \to \mathcal{X}$, and $\mathbb{G}$-symmetric modeling space $\mathcal{X}$, the Koopman operator $\mathsf{X}_{\Delta t}$ (eq. (2)) is $\mathbb{G}$-equivariant and globally optimal by construction. Hence, by Thm. 3, it decomposes into k Koopman operators characterizing the dynamics of each isotypic subspace. Furthermore, for each eigenpair (λ, ψ) of $\mathsf{X}_{\Delta t}$ and every $g \in \mathbb{G}$, the function $\psi_g := \psi(g \diamond (\cdot)) \colon \Omega \to \mathbb{C}$ is also an eigenfunction of $\mathsf{X}_{\Delta t}$ in the same eigenspace,

$$\lambda\, \psi_g(\boldsymbol{\omega}) = \lambda\, \psi(g \diamond \boldsymbol{\omega}) = [\mathsf{X}_{\Delta t}\, \psi](g \diamond \boldsymbol{\omega}) = \psi(\Phi_\Omega(g \diamond \boldsymbol{\omega}, \Delta t)) = \psi(g \diamond \Phi_\Omega(\boldsymbol{\omega}, \Delta t)) = [\mathsf{X}_{\Delta t}\, \psi_g](\boldsymbol{\omega}),$$

implying that the Koopman eigenspaces are $\mathbb{G}$-symmetric spaces. Thus, applying the isotypic decomposition to each eigenspace (Thm. 1) captures the relation of the temporal evolution of eigenfunctions with distinct symmetries (encoded by the *irreps*) via Koopman eigenvalues (see Fig. 3-e). This global decomposition of the dynamics in isotypic subspaces and its symmetry-aware spectral decomposition is referred to as *dynamic harmonic analysis* (DHA). As we show in Secs. 4 and 5, DHA can be leveraged to learn data-driven approximations of the $\mathbb{G}$-equivariant Koopman operator.

4. $\mathbb{G}$-symmetric data-driven Koopman models

The Koopman operator formalism, while practically unfeasible, has inspired numerous data-driven models, aiming to approximate the linear dynamics of the infinite-dimensional Koopman model with a finite-dimensional one built from data (Brunton et al., 2022). This machine learning process uses a dataset of state trajectories, $(\boldsymbol{\omega}_t)_{t=1}^{n}$, to find the relevant observable functions $x_j \colon \Omega \to \mathbb{C}$, $j = 1, \ldots, \ell$, that identify the (latent) observable space $\mathcal{X} := \{x_v := \langle \boldsymbol{x}(\cdot), v \rangle = \sum_{j=1}^{\ell} v_j x_j \mid v \in$

$\mathbb{C}^\ell\}$ on which the Koopman operator $\mathsf{X}\colon \mathcal{X} \to \mathcal{X}$ is approximated by a matrix $\mathsf{W}^* \in \mathbb{C}^{\ell\times\ell}$ as $\mathsf{X}\colon x_v = \langle \boldsymbol{x}(\cdot), v\rangle \mapsto x_{\mathsf{W}^*v} = \langle \boldsymbol{x}(\cdot), \mathsf{W}^*v\rangle = \langle \mathsf{W}\boldsymbol{x}(\cdot), v\rangle$. This approach is based on the fact that if the state representation is built from Koopman eigenfunctions, then $\mathcal{X}$ is an invariant function space of the Koopman operator. Hence, as the latent dimension ℓ increases, the operator X progressively approximates the true Koopman operator (Kostic et al., 2022).

Among different approaches to building Koopman data-driven models, we focus on the deep learning architecture Dynamics Auto-Encoder (DAE) (Lusch et al., 2018). This architecture parameterizes the state representation (encoder) $\boldsymbol{x} : \Omega \to \mathcal{X}$ and its inverse (decoder) $\boldsymbol{x}^{-1} : \mathcal{X} \to \Omega$ as trainable neural networks. Likewise, W is parameterized as a trainable matrix. The cost function for DAE is composed of a reconstruction loss (encouraging injectivity of $\boldsymbol{x}$), a state prediction error, and a latent state prediction error (encouraging the minimization of the modeling error):

$$\mathcal{C}_{\text{DAE}}(\boldsymbol{\omega}_t, H) = \underbrace{||\boldsymbol{x}^{-1}(\boldsymbol{x}(\boldsymbol{\omega}_t)) - \boldsymbol{\omega}_t||^2}_{\text{reconstruction}} + \sum_{h=1}^{H} \Big[\underbrace{||\boldsymbol{x}^{-1}(\mathsf{W}^h\boldsymbol{x}(\boldsymbol{\omega}_t)) - \boldsymbol{\omega}_{t+h}||^2}_{\text{state prediction}} + \gamma \underbrace{||\mathsf{W}^h\boldsymbol{x}(\boldsymbol{\omega}_t) - \boldsymbol{x}(\boldsymbol{\omega}_{t+h})||^2}_{\text{err}_{\boldsymbol{\omega}_t}(\boldsymbol{x},\mathsf{X})\text{: linear prediction}}\Big].$$

Because the DAE architecture assumes that data samples are equally spaced in time, they denote $\mathbb{T} = \mathbb{N}_0$ and $_\Delta t = 1$. Thus, the cost function is defined over a prediction horizon in steps $H \ll n$, and γ balances the error in $\mathcal{X}$ with the error in Ω.

The Equivariant DAE (eDAE) We propose several modifications to the DAE architecture to learn $\mathbb{G}$-symmetric Koopman models and exploit the isotypic decomposition of $\mathcal{X}$ and X. First, we ensure the latent modeling space $\mathcal{X}$ is $\mathbb{G}$-symmetric. This necessitates that the state representation $\boldsymbol{x} : \Omega \to \mathcal{X}$ is a $\mathbb{G}$-equivariant map: $\rho_{\mathcal{X}}(g)\boldsymbol{x}(\boldsymbol{\omega}) = \boldsymbol{x}(g\diamond\boldsymbol{\omega}) \mid \forall\, g \in \mathbb{G}, \boldsymbol{\omega} \in \Omega$, which appropriately translates the symmetric equivalence between states into the latent modeling space (refer to eq. (4)). To achieve this, we define the group representation $\rho_{\mathcal{X}} \sim \rho_{reg} \oplus \rho_{reg} \oplus \cdots \oplus \rho_{reg}$ as the direct sum of $\ell/|G|$ copies of the group regular representation. This ensures that, regardless of the learned observable functions, the basis elements of $\mathcal{X}$ are constrained to transform according to $\mathbb{G}$. We utilize the escnn library (Cesa et al., 2021) to parameterize the state representation $\boldsymbol{x}$ (encoder), and its inverse $\boldsymbol{x}^{-1}$ (decoder) as trainable $\mathbb{G}$-equivariant neural networks.

According to Prop. 2, an optimal linear model will possess a $\mathbb{G}$-equivariant operator X if the modeling space $\mathcal{X}$ is $\mathbb{G}$-symmetric. To ensure this, we parameterize the approximation of the Koopman operator as a $\mathbb{G}$-equivariant matrix, $\rho_{\mathcal{X}}(g)\mathsf{W} = \mathsf{W}\rho_{\mathcal{X}}(g) \mid \forall\, g \in \mathbb{G}$. This parametrization guarantees that any learned linear model will inherently be a $\mathbb{G}$-symmetric model. To exploit the properties of the isotypic basis, we apply the appropriate change of basis to the representation $\rho_{\mathcal{X}}$, exposing the isotypic subspaces $\mathcal{X} = \bigoplus_{i=1}^{k}\mathcal{X}_i$, and their associated group representations $\rho_{\mathcal{X}} = \bigoplus_{i=1}^{k}\rho_{\mathcal{X}_i} \mid \rho_{\mathcal{X}_i} := \bigoplus_{j=1}^{m_i}\bar{\rho}_i$ (refer to Thm. 1). This ensures the output of the learned state representation readily encodes the components in each isotypic subspace $\boldsymbol{x}(\boldsymbol{\omega}_t) := \boldsymbol{x}^{(1)}(\boldsymbol{\omega}_t)\oplus^{\perp}\cdots\oplus^{\perp}\boldsymbol{x}^{(k)}(\boldsymbol{\omega}_t)$. In this basis, the $\mathbb{G}$-equivariant operator X, and its approximation W^*, decompose in block-diagonal form $\mathsf{X} := \bigoplus_{i=1}^{k}\mathsf{X}_i$ (Thm. 3), where each X_i will be approximated by a $\mathbb{G}$-equivariant matrix $\mathsf{W}_i^* : \mathcal{X}_i \to \mathcal{X}_i$ characterizing the dynamics on the isotypic subspace.

After training, this parametrization of the model facilitates a data-driven DHA (Sec. 3). Indeed, if $(\lambda, \boldsymbol{v})$ is an eigenpair of the matrix W_i^*, then $x_{\boldsymbol{v}}^{(i)} := \langle \boldsymbol{x}^{(i)}(\cdot), \boldsymbol{v}\rangle$ becomes an eigenfunction of the model in the isotypic subspace $\mathcal{X}_i$, i.e., $\mathsf{X}_i x_{\boldsymbol{v}}^{(i)} = \lambda x_{\boldsymbol{v}}^{(i)}$. Thus by decomposing all operators X_i, we identify the temporal relation between eigenfunctions in each isotypic subspace, describing how they superimpose in time, as depicted in Fig. 3-e.

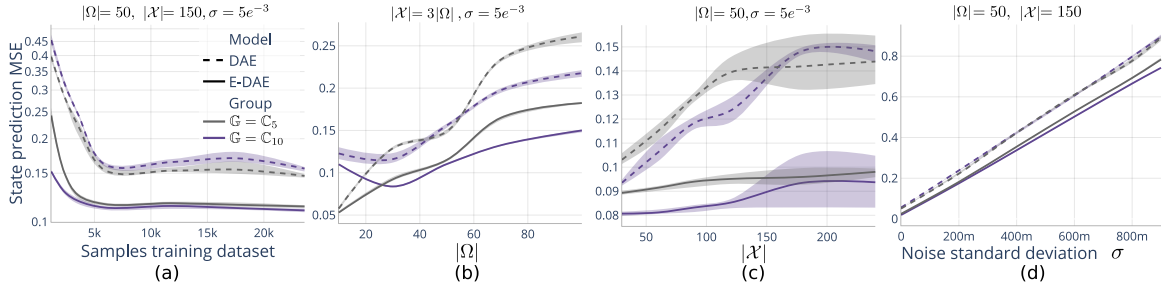

Figure 2: Test set prediction mean square error (MSE) of learned Koopman models (DAE and eDAE) for synthetic systems with symmetry groups $\mathbb{C}_5$ and $\mathbb{C}_{10}$, varying state dimension $|\Omega|$, latent model space dimension $\ell = |\mathcal{X}|$, and noise variance σ. Solid lines and shaded areas represent the mean, maximum, and minimum prediction error among 4 training seeds. (a) MSE vs. training samples. (b) MSE over varying state dimension. (c) MSE over varying dimensionality of the latent model space. (d) MSE over varying noise variance σ.

5. Experiments and results

We present two experiments comparing the performance between equivariant and non-equivariant Koopman models using the DAE and eDAE architectures outlined in the last section. For all of our experiments we set $\gamma = \sqrt{|\mathcal{X}|/|\Omega|}$ to equally balance the error in a dimension of $\mathcal{X}$ with that in a dimension of Ω, a strategy we found effective in practice.

Synthetic symmetric dynamical systems with finite state symmetry groups In this experiment, we model synthetic nonlinear symmetric dynamical systems with arbitrary state symmetry groups $\mathbb{G}$. The systems are designed as constrained stable linear stochastic systems $\boldsymbol{\omega}_{t+\Delta t} = \mathsf{A}_{\Delta t}\boldsymbol{\omega}_t + \boldsymbol{\epsilon}$, $\mathsf{C}\boldsymbol{\omega}_t \geq \boldsymbol{c}$, where $\boldsymbol{\omega} \in \Omega \subseteq \mathbb{R}^n$ is the numerical representation of the system state, $\mathsf{A}_{\Delta t} \in \mathbb{R}^{n\times n}$ the linear dynamics matrix, $\boldsymbol{\epsilon} \in \mathbb{R}^n$ is a white-noise stochastic process with standard deviation σ, and $\mathsf{C} \in \mathbb{R}^{n_c\times n}, \boldsymbol{c} \in \mathbb{R}^{n_c}$ the parameters describing n_c inequality constraints on the dynamics. These systems are $\mathbb{G}$-symmetric if $\mathsf{A}_{\Delta t}$ is $\mathbb{G}$-equivariant $\rho_{\mathbb{R}^n}(g)\mathsf{A}_{\Delta t} = \mathsf{A}_{\Delta t}\rho_{\mathbb{R}^n}(g) \mid \forall\ g \in \mathbb{G}$ and any constraint is also enforced for all symmetric states $\boldsymbol{C}_{k,:}\ g \diamond \boldsymbol{\omega} \geq \boldsymbol{c}_k \mid \forall\ k \in [1, n_c], g \in \mathbb{G}$.

These synthetic systems allow us to evaluate the impact of symmetry exploitation in learning Koopman models for arbitrary groups $\mathbb{G}$, system's dimensionality $|\Omega|$, dimensionality of the Koopman model latent state $|\mathcal{X}|$, and standard deviation σ of the noise. The experiment results demonstrate that the eDAE architecture yields superior models in terms of sample efficiency and generalization (Fig. 2-a), decreased sensitivity to the system's dimensionality $|\Omega|$ (Fig. 2-b), reduced sensitivity to the dimensionality of the latent model space $\ell = |\mathcal{X}|$ (Fig. 2-c), and slightly improved robustness to noise (Fig. 2-d).

Modeling quadruped closed-loop dynamics In this experiment, we investigate the use of a Koopman model for robot dynamics, while quantifying the impact of symmetry exploitation. The focus is on modeling the closed-loop dynamics of the mini-cheetah quadruped robot's locomotion on mildly uneven terrain. The training data comprises a few trajectories of motion executed by a $\mathbb{G}$-equivariant model predictive controller tracks a desired target base velocity with a fixed trotting periodic gait (Amatucci et al., 2022). As a result, the closed-loop dynamics are $\mathbb{G}$-equivariant (Ordonez-Apraez et al., 2023, eq. (3-4)) and stable, with a limit-cycle trajectory describing the gait cycle and transient dynamics governed by the controller's correction for tracking errors. The state of the system is numerically represented as $\boldsymbol{\omega}_t = [\boldsymbol{q}_{js,t}, \dot{\boldsymbol{q}}_{js,t}, z_t, \boldsymbol{o}_t, \boldsymbol{v}_{\text{err},t}, \boldsymbol{w}_{\text{err},t}] \in \Omega \subseteq \mathbb{R}^{46}$, com-

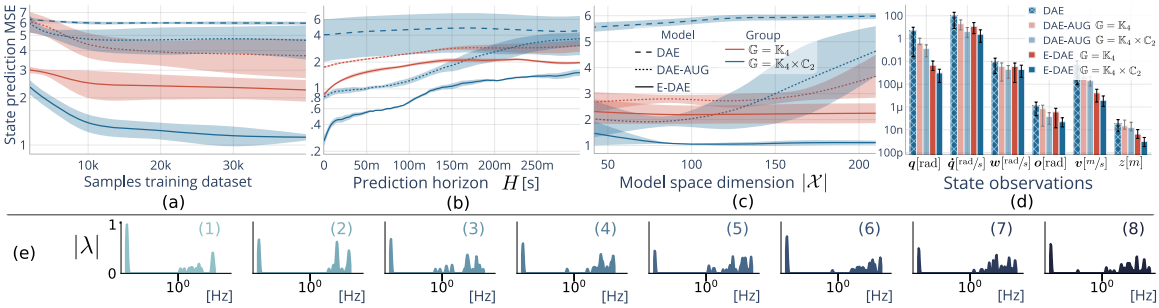

Figure 3: Test set prediction mean square error (MSE) of learned Koopman models (DAE, DAE$_{aug}$, and eDAE) for the mini-cheetah robot's closed-loop dynamics, comparing the use of the symmetry group $\mathbb{G} = \mathbb{K}_4 \times \mathbb{C}_2$ and the subgroup $\mathbb{G} = \mathbb{K}_4$. Solid lines and shaded areas represent the mean, maximum, and minimum prediction error among 4 training seeds. (a) MSE vs. training samples. (b) MSE vs. prediction horizon. (c) MSE for varying dimensionality of the latent model space $\ell = |\mathcal{X}|$. (d) MSE of measurable state observables in original units. (e) Eigenvalue power spectrum from the eDAE Koopman operators for each of the 8 isotypic subspaces. The frequency of oscillation of a mode is given by $\text{Arg}(\lambda)/(2\pi\Delta t)$ (horizontal axis) and the decay rate of the mode by $|\lambda|^{1/\Delta t}$.

posed of the joint-space generalized position $\boldsymbol{q}_{js} \in \mathcal{Q}_{js} \subseteq \mathbb{R}^{24}$, and velocity $\dot{\boldsymbol{q}}_{js} \in \mathcal{T}_{\boldsymbol{q}}\mathcal{Q}_{js} \subseteq \mathbb{R}^{12}$ coordinates, base height $z_t \in \mathbb{R}^1$, base orientation quaternion $\boldsymbol{o} \in \mathbb{R}^4$, and the error in the desired linear and angular base velocities $\boldsymbol{v}_{\text{err},t} \in \mathbb{R}^3$ and $\boldsymbol{w}_{\text{err},t} \in \mathbb{R}^3$, respectively.

The full symmetry group of this robot is $\mathbb{G} = \mathbb{K}_4 \times \mathbb{C}_2$, of order 8 (see symmetric states). This implies that the system's set of states can be decomposed into 8 copies of the quotient set of unique states $\Omega \,/\, \mathbb{G}$ (Sec. 3). Thus, for this system, symmetry exploitation is crucial to mitigate the effects of the curse of dimensionality and potential bias of the training dataset, implying that data is sampled not-uniformly across the 8 quotient sets. The results show a clear superior performance of the $\mathbb{G}$-equivariant Koopman models (eDAE), over the models trained with data-augmentation DAE$_{aug}$, and no symmetry exploitation (DAE) in terms of sample-efficiency (Fig. 3-a), forecasting error (Fig. 3-b-d), and robustness to hyper-parameter's variation (Fig. 3-c). Furthermore, models trained by exploiting the system's entire symmetry group $\mathbb{K}_4 \times \mathbb{C}_2$ constantly outperform those exploiting only the subgroup $\mathbb{K}_4$. Lastly, we highlight the advantage of the learned eDAE Koopman models by leveraging DHA. Since $\mathbb{G}$ is an Abelian group, the modeling space will decompose into 8 isotypic subspaces. Thus, the learned dynamics are characterized as the superposition of relevant symmetric dynamic modes from each isotypic subspace (see Fig. 1-b), that is, eigenvectors $\boldsymbol{v}^{(i)} \in \mathcal{X}_i$ with temporal dynamics given by an eigenvalue λ. We summarize the learned temporal dynamics of these symmetric modes with the power spectrum of each isotypic subspace in Fig. 3-e.

6. Conclusions

We introduced the use of harmonic analysis for decomposing and understanding the dynamics of symmetric robotic systems. By partitioning the state space into isotypic subspaces, we have shown how complex motions can be characterized as the superposition of lower-dimensional, symmetric and synergistic motions. This entails the decomposition of (local and global) linear models of the system's dynamics into independent models for each subspace. Leveraging this, we learn a data-driven global linear model using a novel equivariant deep-learning architecture to approximate the Koopman operator. The method's practical validity is evidenced by presenting the first successful attempt to learn a liner model of the closed-loop dynamics of a quadruped robot's locomotion.

Acknowledgments

This work was supported in part by PNRR MUR Project PE000013 CUP J53C22003010006 "Future Artificial Intelligence Research (hereafter FAIR)", funded by the European Union – NextGenerationEU

References

Ian Abraham and Todd D Murphey. Active learning of dynamics for data-driven control using koopman operators. IEEE Transactions on Robotics, 35, 2019.

Angelo Alessandri, Marco Baglietto, and Giorgio Battistelli. Receding-horizon estimation for discrete-time linear systems. IEEE Transactions on Automatic Control, 48, 2003.

Lorenzo Amatucci, Joon-Ha Kim, Jemin Hwangbo, and Hae-Won Park. Monte carlo tree search gait planner for non-gaited legged system control. In International Conference on Robotics and Automation (ICRA), 2022.

H Harry Asada. Global, unified representation of heterogenous robot dynamics using composition operators: A koopman direct encoding method. IEEE/ASME Transactions on Mechatronics, 2023.

Daniel Bruder, Xun Fu, R Brent Gillespie, C David Remy, and Ram Vasudevan. Data-driven control of soft robots using koopman operator theory. IEEE Transactions on Robotics, 37, 2020.

Steven L. Brunton, Marko Budišić, Eurika Kaiser, and J. Nathan Kutz. Modern koopman theory for dynamical systems. SIAM Review, 64, 2022.

Gabriele Cesa, Leon Lang, and Maurice Weiler. A program to build e (n)-equivariant steerable cnns. In International Conference on Learning Representations, 2021.

Mildred S Dresselhaus, Gene Dresselhaus, and Ado Jorio. Group theory: application to the physics of condensed matter. Springer Science & Business Media, 2007.

R. Featherstone. Rigid Body Dynamics Algorithms. Springer-Verlag, Berlin, Heidelberg, 2007.

Carl Folkestad and Joel W Burdick. Koopman nmpc: Koopman-based learning and nonlinear model predictive control of control-affine systems. In IEEE International Conference on Robotics and Automation (ICRA), 2021.

Martin Golubitsky, Ian Stewart, and David G Schaeffer. Singularities and Groups in Bifurcation Theory: Volume II, volume 69. Springer Science & Business Media, 2012.

Irina Higgins, Sébastien Racanière, and Danilo Rezende. Symmetry-based representations for artificial and biological general intelligence. Frontiers in Computational Neuroscience, 16, 2022.

Anthony W. Knapp. Representation Theory of Semisimple Groups, An Overview Based on Examples (PMS-36). Princeton University Press, Princeton, 1986.

Marin Kobilarov, Duy-Nguyen Ta, and Frank Dellaert. Differential dynamic programming for optimal estimation. In IEEE International Conference on Robotics and Automation (ICRA), 2015.

Milan Korda and Igor Mezić. Linear predictors for nonlinear dynamical systems: Koopman operator meets model predictive control. Automatica, 93, 2018.

Vladimir Kostic, Pietro Novelli, Andreas Maurer, Carlo Ciliberto, Lorenzo Rosasco, and Massimiliano Pontil. Learning dynamical systems via Koopman operator regression in reproducing kernel hilbert spaces. In Advances in Neural Information Processing Systems, 2022.

Vladimir R Kostic, Pietro Novelli, Riccardo Grazzi, Karim Lounici, and Massimiliano Pontil. Deep projection networks for learning time-homogeneous dynamical systems. arXiv preprint arXiv:2307.09912, 2023.

Cornelius Lanczos. The variational principles of mechanics. Courier Corporation, 2012.

Andrzej Lasota and Michael C. Mackey. Chaos, Fractals, and Noise, volume 97 of Applied Mathematical Sciences. Springer New York, 1994.

Weiwei Li and Emanuel Todorov. Iterative linear quadratic regulator design for nonlinear biological movement systems. In First International Conference on Informatics in Control, Automation and Robotics, volume 2. SciTePress, 2004.

Bethany Lusch, J Nathan Kutz, and Steven L Brunton. Deep learning for universal linear embeddings of nonlinear dynamics. Nature communications, 9, 2018.

Carlos Mastalli, Rohan Budhiraja, Wolfgang Merkt, Guilhem Saurel, Bilal Hammoud, Maximilien Naveau, Justin Carpentier, Ludovic Righetti, Sethu Vijayakumar, and Nicolas Mansard. Crocoddyl: An efficient and versatile framework for multi-contact optimal control. In IEEE International Conference on Robotics and Automation (ICRA), 2020.

Alexandre Mauroy, Y Susuki, and I Mezić. Koopman operator in systems and control. Springer, 2020.

David Mayne. A second-order gradient method for determining optimal trajectories of non-linear discrete-time systems. International Journal of Control, 3, 1966.

Afshin Mesbahi, Jingjing Bu, and Mehran Mesbahi. On modal properties of the koopman operator for nonlinear systems with symmetry. In American Control Conference (ACC), 2019.

Sean P. Meyn and Richard L. Tweedie. Markov Chains and Stochastic Stability. Communications and Control Engineering. Springer London, 1993.

Igor Mezić. Koopman operator, geometry, and learning of dynamical systems. Not. Am. Math. Soc., 68, 2021.

Frank Noé and Feliks Nuske. A variational approach to modeling slow processes in stochastic dynamical systems. Multiscale Modeling & Simulation, 11, 2013.

Daniel F Ordonez-Apraez, Mario Martin, Antonio Agudo, and Francesc Moreno. On discrete symmetries of robotics systems: A group-theoretic and data-driven analysis. In Proceedings of Robotics: Science and Systems, Daegu, Republic of Korea, July 2023.

Anastasiya Salova, Jeffrey Emenheiser, Adam Rupe, James P Crutchfield, and Raissa M D'Souza. Koopman operator and its approximations for systems with symmetries. Chaos: An Interdisciplinary Journal of Nonlinear Science, 29, 2019.

Subhrajit Sinha, Sai Pushpak Nandanoori, and Enoch Yeung. Koopman operator methods for global phase space exploration of equivariant dynamical systems. IFAC-PapersOnLine, 53, 2020.

Vivian T Steyert. Uncovering Structure with Data-driven Reduced-Order Modeling. PhD thesis, Princeton University, 2022.

Amit Surana. Koopman framework for nonlinear estimation. The Koopman Operator in Systems and Control: Concepts, Methodologies, and Applications, 2020.

Yuval Tassa, Nicolas Mansard, and Emo Todorov. Control-limited differential dynamic programming. In IEEE International Conference on Robotics and Automation (ICRA), pages 1168–1175. IEEE, 2014.

Xinglong Zhang, Wei Pan, Riccardo Scattolini, Shuyou Yu, and Xin Xu. Robust tube-based model predictive control with koopman operators. Automatica, 137, 2022.